



HAL
open science

Physico-chemical and spectroscopic quality assessment of compost issued from date palm waste valorization

Wadii Abid, Imen Ben Mahmoud, Saoussan Masmoudi, Mohamed Ali Triki,
Stéphane Mounier, Emna Ammar

► To cite this version:

Wadii Abid, Imen Ben Mahmoud, Saoussan Masmoudi, Mohamed Ali Triki, Stéphane Mounier, et al.. Physico-chemical and spectroscopic quality assessment of compost issued from date palm waste valorization. *Journal of Environmental Management*, 2020, 264, pp.110492. 10.1016/j.jenvman.2020.110492 . hal-02559715

HAL Id: hal-02559715

<https://hal.science/hal-02559715>

Submitted on 30 Apr 2020

HAL is a multi-disciplinary open access archive for the deposit and dissemination of scientific research documents, whether they are published or not. The documents may come from teaching and research institutions in France or abroad, or from public or private research centers.

L'archive ouverte pluridisciplinaire **HAL**, est destinée au dépôt et à la diffusion de documents scientifiques de niveau recherche, publiés ou non, émanant des établissements d'enseignement et de recherche français ou étrangers, des laboratoires publics ou privés.

28biodegradation and mineralization. A total of 12 fluorescence excitation emission matrices
29of composts were successfully decomposed into a four-factor model using PARAFAC
30analysis. For the 4 main evidenced components, the excitation/emission (Ex/Em) wavelengths
31were of 350/450 nm, 400/500 nm 450/530 nm and 325/400 nm attributable respectively to
32humic-like and fulvic-like substances.

33**Keywords:** Date palm waste, goat manure, compost, FTIR, fluorescence spectroscopy,
34PARAFAC analysis.

35

136Introduction

37

38 At present, organic waste valorization is an important strategy for human and environment
39safeguard, reducing agricultural costs and chemical products use. Composting was considered
40as an effective biological, economical and sustainable process to reuse the organic matter
41wastes (Sellami et al., 2008; Hachicha et al., 2009a; Masmoudi et al., 2013; El Fels et al.,
422016). Indeed, the composting process stabilizes the organic waste by its conversion into
43humic substances and inactivate pathogens, allowing compost use for soil amendment
44(Hachicha et al., 2006; Zhang and Sun, 2015). Several studies had developed the organic
45agricultural wastes composting such as olive mill waste (Hachicha et al., 2006; Hachicha et
46al., 2008; Masmoudi et al., 2013), sludge issued from the olive mill waste evaporation ponds
47and poultry manure (Hachicha et al., 2009b), horticultural wastes (Gavilanes-Terán et al.,
482015), green waste (Abid et al., 2015; Zhang and Sun, 2015) and *Acacia* residues (Brito et al.,
492015). Consequently, the composting process and the final product quality depend on many
50factors such as the raw materials nature and their formulation, the windrow and the ambient
51temperatures, the windrow materials water content and returning frequency and the microbial
52activity (Masmoudi et al., 2013; Cesaro et al., 2015). Previous studies established that

53compost quality was especially related to its stability and maturity (Hachicha et al., 2009a;
54Cesaro et al., 2015; Nikaeen et al., 2015). Further, compost quality was assessed with
55different physico-chemical (pH, electrical conductivity (CE), carbon measure, C/N,
56temperature and moisture) and biological (microbial population, respiration, germination
57index, solvitan test) parameters, associated to spectroscopic techniques (FTIR, UV-visible and
58fluorescence spectroscopy) (Sellami et al., 2008; Yu et al., 2011; Masmoudi et al., 2013; El
59Fels et al., 2014; Mehta et al., 2014; Song et al., 2015; Kulikowska, 2016).

60 In the Mediterranean basin, date palm is largely cultivated. Indeed, in Tunisia, there are
61more than 4.5 million trees producing an important waste quantities essentially palm leaf
62waste (16 kg/tree yearly) (Ben Salah, 2014).

63 In the present study, an industrial ecological interest was considered in the date palm waste
64valorization by its co-composting with goat manure and compost quality assessment, using
65physico-chemical and biological parameters associated to spectroscopic techniques (FTIR,
66UV-visible and fluorescence spectroscopy) to evaluate the organic matter biodegradation. The
67final product availability would contribute to a sustainable development.

68

69 **2. Materials and methods**

70

71 *2.1. Composting procedure*

72

73 In this study, goat manure and crushed date palm waste composed essentially of palm
74leaflets both collected from the Oasis of Cheneni-Gabes (South of Tunisia) were used for the
75composting procedure. The physico-chemical characteristics of the mentioned materials are
76presented in Table 1.

77 The composting procedure was carried out at the Chenini Oasis Protection Association
78composting site, as described in Abid et al. (2016). The windrow was watered with the
79previous date palm waste soaking-water, characterized by ~~aeidie~~low pH (5.83) and its
80important EC (5.61 mS cm⁻¹) and mesophilic flora (4.1 x 10⁷ ufc mL⁻¹) to keep a moisture
81range of around 50%.

82 During the composting procedure, homogeneous and representative samples were collected
83from the windrow and refrigerated until analysis. Each sample consists of a mixture of 9 sub-
84samples taken at different points of the windrow. Before analysis, the samples were dried at
85105 °C, and then mechanically crushed to obtain homogeneous powder.

86

~~287~~ *Physico-chemical analysis*

88

89 The windrow temperature was measured using digital thermometer (type Alla, France)
90weekly during the mesophilic and the thermophilic composting phases and monthly until its
91maturity. The presented temperature value consists of a mean of 12 measurements at different
92points and depths of the windrow.

93 All the dried and crushed samples were submitted to physico-chemical analysis using
94standard methods. The pH and EC values were measured in a solution consisting of 20 g of
95sample in 100 ml of distilled water. Organic matter (OM) was determined by dry matter and
96weight loss on ignition at 550 °C for 4 h in a muffle furnace (Hachicha et al., 2009b). The
97total Kjeldahl nitrogen (TKN) was determined according to AFNOR (1981). Phosphorus
98content, macro and micro elements were determined using standard methods as mentioned in
99our previous study (Abid et al., 2016).

100

~~101~~ *Dissolved organic matter extraction (DOM)*

102

103 The organic matter extraction was achieved according to Song et al. (2015) with a slight
104 modification. All the dried compost samples were dissolved in distilled water (solid to water
105 ratio of 1:10, w/v) for 24 h in a rotary shaker (Heidolph reax 20) at room temperature. The
106 suspensions were then centrifuged at 5000 rpm for 15 min, filtered through a 0.22 µm
107 membrane filter and refrigerated until spectroscopy analysis. The Dissolved Organic
108 Carbon (DOC) was measured using multi TOC/TN analyzer type (Analytic Jena multi N/C
109 2100S).

110

111 2.4.

Biological analysis

112

2.4.13 Microbial respiration

114

115 Microbial respiration was assayed according to Pallo et al. (2009) and Yu et al. (2011) with
116 some modifications. A sample of 50 g compost was incubated for 24 h in bottle of 1 L where
117 a tube containing 10 mL of NaOH (0.1 N) was placed. The bottles have the same windrows
118 temperature when the sample was collected. The method involves the CO₂ trapping by sodium
119 hydroxide (0.1 N NaOH), and then titration with hydrochloric acid (0.1 N HCl) with the
120 phenolphthalein as a pH indicator. The amount of CO₂ released (C-CO₂) is given by the
121 following formula:

$$122 \text{CO}_2\text{-C (mg /50 g of compost)} = (\text{Control } V_{\text{HCl}} - \text{Sample } V_{\text{HCl}}) \times 2.2;$$

123 Control V_{HCl} (ml): the volume of HCl (0.1 N) used for the titration of NaOH in the control;

124 sample V_{HCl} (ml): the volume of HCl (0.1 N) used for compost sample titration; 2.2 = a

125 coefficient corresponding to 1 mL of HCl (0.1 N) CO₂ (g) determined.

126

127 4.2. *Microbial counts*

128

129 The microbial count was achieved by number of colony forming units count (cfu). A 10 g
130 mass of matured compost was suspended in 90 mL of a sterile peptone water solution and
131 stirred at 150 rpm for 10 min at 28 °C. The suspension was used for serial successive decimal
132 dilutions (10^{-1} to 10^{-7}) and 1 mL was used to inoculate Plate Count Agar medium (PCA). The
133 cell enumeration was for 72 h \pm 4 h at 37 °C \pm 1 °C (Hachicha et al., 2006).

134

135 4.3. *Phytotoxicity test*

136

137 The compost phytotoxicity was evaluated using the germination index (GI) according to
138 the method described by Cesaro et al. (2015). This was determined as follows: 20 g of dry
139 weight compost were extracted with 200 mL of distilled water, stirred for 2 h and then
140 centrifuged at 9000 rpm. Ten *Lipidium sativum* seeds were evenly distributed on filters papers
141 in Petri dishes (10 cm diameter) and moistened with 10 mL of the compost extract. For each
142 sample, three replicate dishes were incubated at 25 °C for three days in the dark. The numbers
143 of germinating seeds per dishes were counted and the length of each seed root was measured.
144 For the control, 10 mL of distilled water were used to moisten the filter. The GI was
145 calculated using the following formula:

146 $GI (\%) = [(Seed\ germination \times Treated\ root\ length) / (Seed\ germination \times Control\ root\ length)]$
147 $\times 100.$

148

149 2.5. *Spectral analysis*

150

151 5.1. *UV-visible*

152

153 The Dissolved Organic Matter (DOM) UV absorbance measurements from 200 to 800 nm
154 were recorded on the Shimadzu UV-1800 spectrophotometer. The base line was carried out
155 with osmosis water used for organic matter extraction. The analyses were performed at
156 neutral pH in quartz cuvettes (1 mm path length) at room temperature. The spectra were
157 recorded in the range of 200 to 800 nm. To characterize the DOM, three quality indices were
158 determined: these were Specific Ultraviolet Absorbances (SUVA) at 254 nm (SUVA₂₅₄),
159 269 nm (SUVA₂₆₉) and 280 nm (SUVA₂₈₀). The SUVA₂₅₄, SUVA₂₆₉ and SUVA₂₈₀ were
160 calculated as ABS(254)/DOC, ABS(269)/DOC, and ABS(280)/DOC (Song et al.,
161 2015). The ratio of the absorbance at 250 nm to that at 365 nm (E_2/E_3) was determined to
162 describe the humification process intensity (reference). The ratio of the absorbance at 280 nm
163 to that at 472 nm (E_2/E_4) was used as an indicator of the relative lignin amounts at the
164 beginning of the humification (reference). Finally the ratio between the absorbance at 472 and
165 that at 664 nm (E_4/E_6) was the most indicative parameter related to the humification degree
166 (Sellami et al., 2008).

167

168 5.2. *Fourier transform infrared spectroscopy*

169

170 The dried compost samples were analyzed using an infrared spectrometer type FTIR
171 Nicolet iS50 (Thermo Scientific, USA). The spectra were scanned over a wavenumber range
172 of 4000-400 cm^{-1} with a resolution of 4 cm^{-1} .

173

174 5.3. *Excitation-emission matrix (EEM) fluorescence spectra*

175

176 The EEM spectra were achieved on the DOM of the different samples collected during the
177composting process using a spectrofluorimeter HITACHI F4500 with scanning emission (Em)
178and excitation (Ex) wavelengths spectra from 200 to 800 nm at 10 nm increments and the
179scan speed was set at 2,400 nm·Min⁻¹. Excitation and emission slit were fixed at 10 nm and
180the detector time response in automatic mode. Fluorescence spectroscopy was carried out on
1814 two time diluted extract to ~~avoid~~correct the inner filter effect ~~(Luciani)~~. The obtained
182fluorescent EEM were processed by Parallel Factor analysis (PARAFAC) and
183~~PROGMEEF~~progMEFF interface provided by PROTEE laboratory, Univ. Toulon (France),
184allowing the extraction of the most representative fluorescent components to characterize the
185source and nature of the sample organic matter (Yu et al., 2011; Mouloubou et al., 2016).

186

187 2.6. *Statistical analysis*

188

189 The data were submitted to variance analysis using Portable IBM SPSS statistics version
19019. All analyses were performed in triplicate. Principal component analysis (PCA) was used
191to examine multivariate relationship between the physico-chemical and biological parameters
192progress during composting. Pearson's correlation coefficient (R) was used to evaluate the
193linear correlation between two parameters at a confidence level of 95% ($p < 0.05$).

194

195 **3. Results and discussion**

196

197 3.1. *Composting performance*

198

199 3.1.1. *Temperature profiles*

200

201 Temperature is one of the main parameters used to monitor the composting process. As
202 shown in Figure 1, the temperature profile of the date palm waste and goat manure co-
203 composting was divided into 4 phases: mesophilic, thermophilic, cooling and maturity.

204 During the first 6 days of the composting process, windrow temperature showed a rapid
205 increase and exceeded the 40 °C (Fig. 1). This period, represented mesophilic phase,
206 characterized by the easily degradation of the organic matter by mesophilic microorganisms.
207 After this period, the temperature rose to above 53 °C, corresponding to the thermophilic
208 phase and remained approximately at 50 °C for 7 days. This high temperature enhanced the
209 windrow sanitation (Zhang et al., 2014; Zhang et al., 2015). This temperature increase was
210 due to the intense microbial activity.

211 By the 20th day of composting, the temperature started to decrease announcing the cooling
212 phase, characterized by the mesophilic microorganism colonization which contributed to the
213 cellulose and lignin degradations and the humus formation (El Fels et al., 2014). According to
214 Zhang et al. (2014), the traditional composting requires between 90 and 270 days to produce
215 mature compost. In this study, the maturity was reached after 190 days of composting; this
216 fact may be attributed to the effect of the initial date palm waste soaking step. However, in
217 another study date palm waste composting was held in 14 months (El Ouaquoudi et al., 2015).
218 At the maturity, the temperature was 35 °C. At the 62 and 133 days, the two observed
219 temperature increases were the result of the windrow return reinforcing the aeration, which
220 stimulate the microorganism activity (Gavilanes-Terán et al., 2015). Also, at the maturity
221 phase, the windrow temperature was highly related to the ambient temperature which
222 increased by the summer beginning from the day 62 until the process end.

223

224 1.2. *pH and EC progress*

225

226 During the date palm waste and goat manure co-composting process, the pH value showed
227a high correlation with the composting time ($R^2 = 0.91$) and varied slightly but remained
228globally neutral while an increase in EC value was noticed with a linear model and also high
229correlation with the composting time ($R^2 = 0.89$). However, a pH decrease by 0.43 units was
230registered at day 84 (Table 2). According to the literature, this decrease was explained by the
231raw material degradation essentially lignicellulose, and the organic acids release (Hachicha et
232al., 2008; Tripetchkul et al., 2012; El Fels et al., 2014). After this fluctuation, the pH value
233was stabilized with the humic substances biosynthesis, these acted as pH buffer (El Fels et al.,
2342014). It could be noticed that the pH profile was different from that found by El Fels et al.
235(2014) who mixed palm waste with sewage sludge characterized by an acidic pH. The
236observed difference would be attributed to the composted raw materials typology and
237pretreatment. The mature compost pH value was in the range of the compost standard value
238(between 6 and 7.5), confirming its suitability for agricultural use as specified by Gavilanes-
239Terán et al. (2015).

240 The EC was also measured during the date palm waste co-composting and reflected the
241compost [salinity ion content](#) and its importance for plant growth (Gavilanes-Terán et al., 2015;
242Singh and Kalamdhad, 2015). The EC values increased during composting process from 2.71
243to 4.33 mS cm^{-1} (Table 2) reflecting the OM mineralization and the ammonium ions and
244mineral salts release (El Fels et al., 2014; Gavilanes-Terán et al., 2015).

245

246 1.3. *Organic matter degradation and C/N progress*

247

248 During the composting process, the OM and C/N progress were the important key
249parameter reflecting raw materials biodegradation and transformation. At the process end, the
250OM was reduced by 63% exhibiting the raw materials deterioration and their oxidation to CO_2

251 and H₂O (Table 2). Indeed, the OM was decomposed and transformed by microorganisms to
252 stable humic substances; the change was highlighted by a mass loss (Singh and Kalamdhad,
253 2015). According to Kulikowska et al. (2015), the OM mineralization amount and rate depend
254 on the raw materials chemical composition, and especially the fibers content like lignin. The
255 date palm waste and goat manure co-composting showed an OM loss of 36.58% although in
256 another study El Ouaquoudi et al. (2015) observed an OM loss of 29% and 62% respectively
257 for date palm waste and date palm/couch-grass clipping wastes mixture subjected to
258 composting during 14 months. These results proved the important effects of date palm waste
259 soaking step and goat manure use investigated in this study.

260 Simultaneously, the OM oxidation led to carbon loss and CO₂ release, increasing the total
261 nitrogen content in the medium. In fact, palm waste and goat manure co-composting exhibited
262 a C/N ratio decrease by 3 folds at the process end confirming its maturity (Table 2) (Tian et
263 al., 2012).

264

265 3.2. *Biological parameters evolution*

266

267 3.2.1. *Respiration*

268

269 Respiration was usually used in compost stability and quality assessment as it refers to the
270 microorganisms activity and OM degradation (Varma and Kalamdhad, 2014; Nikaeen et al.,
271 2015). In this experiment, the initial respiration value was low, expressing microorganism
272 adaptation to the environment. After 6 days, the highest respiration value was observed
273 corresponding to thermophilic phase (Fig. 2) with intense microorganisms activity. According
274 to Nikaeen et al. (2015), this activity would be attributed to labile OM availability which
275 stimulates microbial activity. After this stage, the respiration decreased then a second pic was

276observed at day 33 just after the windrow return that stimulated the microbial activity. From
277the day 34 and until the day 190, the respiration decreased slowly to reach 5.53 mg/50 g
278reflecting compost stability (Gómez et al., 2006).

279

280 2.2. Germination index (GI)

281

282 During the composting process, the compost quality of the different collected samples was
283assessed by phytotoxicity control expressed as GI (Fig. 3). For the first 45 days, the GI
284showed fluctuations related to the OM degradation, the organic acids and the ammonia
285releases at relatively high concentrations considered as phytotoxic (Zhang et al., 2014). Also,
286phenols, alkaloids and ketones as well as others flavonic compounds are considered as seed
287germination inhibitory agents (Hachicha et al., 2009a; El Fels et al., 2016). From the 60th day,
288the germination index increased gradually, indicating the toxic compounds reduction and the
289presence of stable humic substances, rich in organic matter synthesized and accumulated
290during the cooling phase (El Fels et al., 2014; El Fels et al., 2016). According to Sellami et al.
291(2008) and Zhang et al. (2014), the final GI value about 89% may reflect compost maturity
292and phytotoxicity lack. According to Gavilanes-Terán et al. (2015) the obtained compost
293characterized with a GI exceeding 50%, could be used in agriculture without any phytotoxic
294effect. The GI followed a linear model with a relatively correlation with time during the
295composting process ($R^2 = 0.89$).

296

297 3.3. Spectral analysis

298

299 3.1. UV-visible spectroscopy

300

301 The UV-visible spectroscopy was used to characterize the DOM, reflecting the organic
302 matter humification during the co-composting of date palm waste and goat manure, as well as
303 the final compost quality. The UV-visible spectra of the initial and final composted materials
304 showed an intensity decrease from the wavelength of 267 to 295 nm (Fig 4). According to
305 Lim et al. (2015), this decrease is related to lignin biodegradation, since the absorbance region
306 around 280 nm is assigned to lignin and aromatic compounds.

307 Different specific ultraviolet absorbance $SUVA_{254}$, $SUVA_{269}$ and $SUVA_{280}$ were calculated
308 (Table 3) and showed respectively an important increase by 2 times, while comparing the
309 initial state (raw materials) to the mature compost. Both of the $SUVA_{254}$ and the $SUVA_{280}$ were
310 relative to the aromatic constituent contents in the DOM (Wang et al., 2013), while the
311 $SUVA_{269}$ was related to lignin derived aromatic carbon (He et al., 2014). The SUVA values
312 increase, confirmed the organic matter degradation and lignin oxidation into aromatic
313 compounds during composting process. In this study, the absorbance ratio E_2/E_3 , E_2/E_4 and E_4/E_6 ,
314 used to control the organic matter biodegradation and humic substances synthesis, varied
315 during the composting process (Table 3); this may be attributed to the organic matter rich in
316 lignin, difficult to be biodegraded. However, in the first 6 composting days, E_4/E_6 decreased
317 because of the mesophilic microorganism activity and increased after the windrow returns to
318 reach 7.40 by the day 21, then decreased successively as a result of raw organic materials
319 humification and humic substances synthesis (Zbytniewski and Buszewski, 2005). By the day
320 84 of composting, the ratio E_4/E_6 increased again after windrow return and then decreased at
321 the end of the process. Wang et al. (2013) found a reduction in E_4/E_6 during the active phase
322 that rose slowly thereafter. According to Zbytniewski and Buszewski (2005), the final E_4/E_6
323 value 5.7 is an index of mature humic acids. More recently, Haddad et al. (2015) had also
324 found an E_4/E_6 ratio value of 6 at the end process of composting olive pomace and cattle
325 manure. They had admitted this ratio as an indicator of humification intensity. Thus, when the

326ratio E_4/E_6 becomes low the compost is mature and humus particles are complexes. Sellami et
327al. (2008) associated the large values of E_4/E_6 ratio to the presence of small size organic
328molecules or more aliphatic structures with high functional groups content. The E_2/E_4 index
329progress presented the same trend as that of the E_4/E_6 ratio during the composting process.
330This ratio intensity would inform on the lignin and other materials at the beginning of
331humification (Zbytniewski and Buszewski, 2005). Furthermore, the observed decreases in $E_2/$
332 E_4 index reflected an intense depolymerisation and microbial monomeric compounds
333degradation (Sellami et al., 2008; Lim and Wu, 2015).

334

335 3.2. FTIR spectroscopy

336

337 The infrared spectroscopy was usually used as a qualitative analysis to identify and monitor
338the chemical groups and bands present in the composted materials, describing the organic
339matter degradation. Figure 5 represents the materials FTIR spectra at various composting
340stages. The major compost FTIR bands are listed in Table 4, where the bands between 4,000
341and 2,000 cm^{-1} were attributed to the humic substances extracted from compost (El Fels et al.,
3422014). At 3,290 cm^{-1} , the pic was more important at the initial composting process than at the
343end, and was assigned to phenol O-H group vibration; this group was degraded during the
344composting process until the compost maturity (Masmoudi et al., 2013). This result is in
345accordance with the phytotoxicity test results. The bands at 2,920 and 2,850 cm^{-1} ,
346characteristic of the aliphatic C-H groups, were more intense at the initial composting
347samples. Indeed, during the composting process, the organic matter was biodegraded and the
348carbon content decreased (El Fels et al., 2014). Also, the bands at 1,690 cm^{-1} attributed to
349C=O group in the organic matter, decreased during composting process by the microbial
350activity. The bands between 1,600 and 900 cm^{-1} were attributed to cellulose and early

351decomposition product (Grube et al., 2006). El Ouaquoudi et al. (2015) had assigned the peak
352at 1,525 cm⁻¹ to lignin considering the date palm waste lignocellulosic material.

353In the region between 1,300 and 1,400 cm⁻¹, the bands were more intense in the final compost
354sample. According to Grube et al. (2006), this region is characteristic of nitrate bands
355appearance, usually detected at the latter composting stage, when raw materials were well
356composted. However, the peak at 1,170 cm⁻¹ was more intense at the initial mixture and was
357attributed to C-O-C groups of cellulose and hemicellulose as reported by Xu et al. (2013) at
3581,160 cm⁻¹. At 1,560 cm⁻¹, the band decreased with the composting time, revealing peptide
359degradation in manure (Hachicha et al., 2009b).

360 The changes in the organic matter content and in aromaticity degree were also assessed by
361the calculation of the 3 absorption ratios 1,650/2,845, 1,525/2,925 and 2,920/1,640 (Table 5).
362During the composting process, the 1,650/2,845 and 1,525/2,925 ratios showed an increase
363while the specific ratio of aliphatic C/aromatic C (2,920/1,640) decreased. These results could
364be explained by an increase in aromaticity and the biosynthesis of aromatic structures, such as
365humic-like and fulvic-like substances, with the decomposition/transformation of aliphatic
366components, polysaccharides, and alcohols (Wu et al., 2011; El Ouaquoudi et al., 2015).

367 These infrared spectroscopy findings were in accordance with those of the physico-chemical
368parameters, both of the data confirmed the date palm waste and goat manure co-composting
369product maturity and quality.

370

371 3.3. Fluorescence spectroscopy

372

373 The three dimensional EEM fluorescence spectra of the DOM composted material progress
374are presented in Figure 6 (A). These spectra were characterized by the presence of a
375fluorophore pipeak having different intensities depending on the composting progress and it

376highest intensity was registered in the final compost spectra after 190 days of composting.
377The variable fluorophore pi peak had an excitation/emission wavelength pairs between 350-
378400 (mean value = 375)/400-500 (mean value = 470) nm, characteristic of humic-like
379substances and high molecular weight (Albretch et al., 2015; Song et al., 2015; Mouloubou et
380al., 2016). According to He et al. (2015), the fluorophores with emission wavelengths
381exceeding 380 nm are ascribed to humic-like species, while those less than 380 nm represent
382protein-like species, such as tyrosine and tryptophan-like species. Based on these data, no
383proteins like fluorophore were detected during the process. Consequently, the total
384luminescence would be issued from the humic-like compounds. However, the humic like
385signal could be generated by a mixture of fluorescent compounds. The ratio of the red zone to
386the total EEM fluorescent area had increased by 76% at the end process revealing the
387formation of humic substances (Figure 6 B). The ratio fluctuation during the first 60 days of
388composting was due to the microbial activity and the degradation of organic matter.

389 As shown in Figure 7, the PARAFAC analysis decomposed the EEM fluorescent spectra
390into 4 fluorophore components (ConcordiaCORCONDIA > 66%). The first component is
391located at 350/450 nm (S1) and it is representative of the humic like compounds. The second
392(S2) is located at 400/500 nm and is less conjugated than the third (S3) one located at 450/530
393nm. These entire three components represent the humic-like group. The fourth (S4) represent
394the fulvic like component with an excitation at 325/400 nm. From S4 to S1 to S2 to S3 we can
395observe a conjugate trend inducing a red shift evolution for both excitation and emission
396wavelengths. Observing the ratio of S3 over S2 contribution during the composting process,
397we may note that the S1 contribution increase more than other components. This is a
398confirmation of the FTIR trend were C=C is increasing during the same time. Moreover,
399considering the increase of the SUVAs, the fluorescence intensity and the GI while COD and

400microbial respiration decreases, we may suggest that at the end of the process (over 120 d),
401both of conjugated carbon and aromaticity increased.

402

403 3.4. *Compost specification*

404

405 The compost prepared with date palm waste and goat manure co-composting was
406characterized by a neutral pH and relatively high EC. It also exhibited a low C/N ratio and a
407high GI value (88%) reflecting its stability (Table 6). Considering its total nitrogen content
408inferior to 3% and organic matter inferior to 55%, the produced compost could be classified
409as vegetal compost (French standards NF U 44-051, 1981).

410After six months of palm waste and goat manure co-composting while comparing to El Fels
411et al. (2014) compost who also studied the palm waste co-composting with sludge, the
412produced compost present higher carbon content than that previously described but a lower
413nitrogen content.

414

415 3.5. *Statistical analysis*

416

417 The correlation matrix between the physico-chemical and the biological parameters
418progress during the composting process (Table 7) and the PCA plan representation (Fig 8)
419showed a significant positive correlation between pH, C/N ratio and OM content. However,
420during the composting process, the organic matter biodegradation decreased and as a result,
421the carbon content was reduced as well as C/N ratio. In addition, temperature and respiration
422were highly correlated revealing that microorganism activity depends on the temperature and
423specificity for each composting stage (mesophilic and thermophilic). Moreover, a negative
424correlation was observed between the germination index and the EC. These are opposed to the

425previous group including OM, pH and C/N. Indeed, the organic acids and the other phytotoxic
426components released during composting process affected the seed germination.

427

428. **Conclusions**

429

430 Date palm waste and goat manure co-composting is an efficient solution providing organic
431matter for a sustainable agriculture. During the composting process, physico-chemical and
432biological parameters were in correlation, proving the organic matter biodegradation and the
433compost produced quality. The use of spectroscopic techniques approved the lignin
434degradation and the humic substance components formation. The obtained compost was
435without phytotoxicity and ready for agriculture application.

436

437**Aknowledgements**

438

439 The authors would like to express their gratitude to the staff at the Oasis Cheninni
440Safeguard Association for their help in providing the material necessary for this study.

441

442**References**

443

444Abid, W., Ammar, E., Triki, M.A., Ben Abbou, M., Elhaji, Mounia., 2015. Gestion et
445 valorisation des margines par co compostage avec les déchets verts et amendements des
446 sols agricoles pour l'amélioration des rendements. Office Marocain de la Propriété
447 Industrielle et Commerciale. MA 20150445 A1.

448Abid, W., Magdich, S., Ben Mahmoud, I., Medhioub, K., Ammar, E., 2016. Date palm wastes
449 co-composted product: an efficient substrate for tomato (*Solanum lycopersicum* L.)
450 seedling production. *Waste Biomass Valor.* pp 1-11. DOI 10.1007/s12649-016-9767-y.

451Albrecht, R., Verrecchi, E., Pfeifer, H.R., 2015. The use of solid-phase fluorescence
452 spectroscopy in the characterization of organic matter transformations. *Talanta* 134, 453-
453 459.

454Ben Salah, M., 2014. Le recyclage des sous-produits des oasis : acquis et perspective.
455 Observatoire du Sahara et du Sahel. 85 p.

456Brito, L.M., Mourão, I., Coutinho, J., Smith, S.R., 2015. Co-composting of invasive *Acacia*
457 *longifolia* with pine bark for horticultural use. *Environ. Technol.* 36, 1632-1642.

458Cesaro, A., Belgiorno, V., Guid, M., 2015. Compost from organic solid waste: Quality
459 assessment and European regulations for its sustainable use. *Resour. Conserv. Recyc.* 94,
460 72–79.

461El Fels, L., Zamama, M., El Asli, A., Hafidi, M., 2014. Assessment of biotransformation of
462 organic matter during co-composting of sewage sludge-lignocelulosic waste by
463 chemical, FTIR analyses, and phytotoxicity tests. *Int. Biodeter. Biodegr.* 87, 128-137.

464El Fels, L., Hafidi, M., Ouhdouch, Y., 2016. *Artemia salina* as a new index for assessment of
465 acute cytotoxicity during co-composting of sewage sludge and lignocellulose waste.
466 *Waste Manage.* 50, 194-200.

467El Ouaquodi, F., El Fels, L., Lemée, L., Amblès, A., Hafidi, H., 2015. Evaluation of
468 lignocellulose compost stability and maturity using spectroscopic (FTIR) and thermal
469 (TGA/TDA) analysis. *Ecol. Eng.* 75, 217–222.

470French Association for Standardization (AFNOR), 1980. Animal feeding stuffs.
471 Determination of total phosphorus content. Spectrophotometric method, NFV18-106. 4 p.

472 French Association for Standardization (AFNOR), 1981. Determination of nitrogen Kjeldahl -
473 Titrimetric determination method after mineralization and distillation, NF T 90-110.

474 Gavilanes-Terán, I., Jara-Samaniego, J., Idrovo-Novillo, J., Bustamante, A., Moral, R.,
475 Paredes, C., 2015. Windrow composting as horticultural waste management strategy – A
476 case study in Ecuador Irene. *Waste Manage.* 48, 127-34.

477 Gómez, R.B., Lima, F.V., Ferrer, A.S., 2006. The use of respiration indices in the composting
478 process: a review. *Waste Manage. Res.* 24, 37-47.

479 Grube, T., Lin, J.G., Lee, P.H., Kokorevicha, S., 2006. Evaluation of sewage sludge-based
480 compost by FTIR spectroscopy. *Geoderma* 130, 324-333.

481 Hachicha, S., Chtourou, M., Medhioub, K., Ammar, E., 2006. Compost of poultry manure and
482 olive mill wastes as an alternative fertilizer. *Agron. Sustain. Dev.* 26, 135–142.

483 Hachicha, S., Sallemi, F., Medhioub, K., Hachicha, R., Ammar, E., 2008. Quality assessment
484 of composts prepared with olive mill wastewater and agricultural wastes. *Waste Manage.*
485 28, 2593–2603.

486 Hachicha, S., Cegarra, J., Sellami, F., Hachicha, R., Drira, N., Medhioub, K., Ammar, E.,
487 2009a. Elimination of polyphenols toxicity from olive mill wastewater sludge by its
488 co-composting with sesame bark. *J. Hazard. Mater.* 161, 1131–1139.

489 Hachicha, S., Sellami, F., Cegarra, J., Hachicha, R., Drira, N., Medhioub, K., Ammar, E.,
490 2009b. Biological activity during co-composting of sludge issued from the OMW
491 evaporation ponds with poultry manure—Physico-chemical characterization of the
492 processed organic matter. *J. Hazard. Mater.* 162, 402–409.

493 Haddad, G., El-Ali, F., Mouneimne, A.H., 2015. Humic matter of compost: Determination of
494 humic spectroscopic ratio (E_4/E_6). *Curr. Sci. Int.* 4, 56-72.

495He, X., Xi, B., Cui, D.Y., Liu, D., Tan, W.B., Pan, H.W., Li, D., 2014. Influence of chemical
496 and structural evolution of dissolved organic matter on electron transfer capacity during
497 composting. *J. Hazard. Mater.* 268, 256–263.

498He, X-S., Xi, B-D., Li, W-T., Gao, R-T., Zhang, H., Tan, W-B., Huang, C-H., 2015. Insight
499 into the composition and evolution of compost-derived dissolved organic matter using
500 high-performance liquid chromatography combined with Fourier transform infrared and
501 nuclear magnetic resonance spectra. *J. Chromatogr. A.* 1420, 83-91.

502Kulikowska, D., 2016. Kinetics of organic matter removal and humification progress during
503 sewage sludge composting. *Waste Manage.* 49, 196-203.

504Lim, S.L., Wu, T.Y., 2015. Determination of maturity in the vermicompost produced from
505 palm oil mill effluent using spectroscopy, structural characterization and
506 thermogravimetric analysis. *Ecol. Eng.* 84, 515–519.

507Masmoudi, S., Jarboui, R., El Feki, H., Gea, T., Medhioub, K., Ammar, E., 2013.
508 Characterization of olive mill wastes composts and their humic acids: stability assessment
509 within different particle size fractions. *Environ. Technol.* 34, 787-797.

510Mehta, C.M., Palni, U., Franke-whittle, I.H., Sharma, A.K., 2014. Compost: its role,
511 mechanism and impact on reducing soil-borne plant diseases. *Waste Manage.* 34, 607-
512 622.

513Mouloubou, O.R., Prudent, P., Mounier, S., Boudenne, J.L., Madi, G.A., Theraulaz, F., 2016.
514 An adapted sequential chemical fractionation coupled with UV and fluorescence
515 spectroscopy for calcareous soil organic matter study after compost amendment.
516 *Microchem. J.* 124, 139-148.

517Nikaeen, M., Nafez, A.H., Bina, B., Nabavi, B.F., Hassanzadeh, A., 2015. Respiration and
518 enzymatic activities as indicators of stabilization of sewage sludge composting. *Waste*
519 *Manage.* 39, 104-111.

520 Pallo, F.J.P., Lemée, L., Ambles, A., 2009. Les lipides libres des sols sous formations
521 naturelles au Burkina Faso: Nature, origine et relation avec quelques facteurs de fertilité.
522 Etude et gestion des sols, 16, 101-112.

523 Singh, J., Kalamdhad, A.S., 2015. Assessment of compost quality in agitated pile composting
524 of water hyacinth collected from different sources. Int. J. Recycl. Org. Waste Agricult. 4,
525 175–183.

526 Sellami, F., Hachicha, S., Chtourou, M., Medhioub, K., Ammar, E., 2008. Maturity
527 assessment of composted olive mill wastes using UV spectra and humification
528 parameters. Bioresour. Technol. 99, 6900–6907.

529 Song, C., Li, M., Xi, B., Wei, Z., Zhao, Y., Jia, X., Qi, H., Zhu, C., 2015. Characterisation of
530 dissolved organic matter extracted from the bio-oxidative phase of co-composting of
531 biogas residues and livestock manure using spectroscopic techniques. Int. Biodeter.
532 Biodegr. 103, 38-50

533 Tian, W., Li, L., Liu, F., Zhang, Z., Yu, G., Shen, Q., Shen, B., 2012. Assessment of the
534 maturity and biological parameters of compost produced from dairy manure and rice
535 chaff by excitation–emission matrix fluorescence spectroscopy. Bioresour. Technol. 110,
536 330–337.

537 Tripetchkul, S., Pundee, K., Koonsrisuk, S., Akeprathumchai, S., 2012. Co-composting of
538 coir pith and cow manure: initial C/N ratio vs physico-chemical changes. Int. J. Recycl.
539 Org. Waste Agricult. 15, 2-8.

540 Varma, S.V., Kalamdhad, A.S., 2014. Stability and microbial community analysis during
541 rotary drum composting of vegetable waste. Int. J. Recycl. Org. Waste Agricult. 52, 2-9.

542 Wang, K., Weiguang, L., Gong, X., Li, Y., Wu, C., Ren, N., 2013. Spectral study of
543 dissolved organic matter in biosolid during the composting process using inorganic
544 bulking agent: UV-vis, GPC, FTIR and EEM. Int. Biodeter. Biodegr. 85, 617-623.

545 Wu, H., Zhao, Y., Long, Y., Zhu, Y., Wang, H., Lu, W., 2011. Evaluation of the biological
546 stability of waste during landfill stabilization by thermogravimetric analysis and Fourier
547 transform infrared spectroscopy. *Bioresour. Technol.* 102, 9403–9408.

548 Xu, F., Yu, J., Tesso, T., Dowell, F., Wang, D., 2013. Qualitative and quantitative analysis of
549 lignocellulosic biomass using infrared techniques: A mini-review. *Appl. Energ.* 104,
550 801–809.

551 Yu, G.H., Wu, M.J., Luo, Y.H., Yang, X.M., Ran, W., Shen, Q.R., 2011. Fluorescence
552 excitation–emission spectroscopy with regional integration analysis for assessment of
553 compost maturity. *Waste Manage.* 31, 1729-1736.

554 Zhang, L., Sun, X., 2014. Changes in physical, chemical, and microbiological properties
555 during the two-stage co-composting of green waste with spent mushroom compost and
556 biochar. *Bioresour. Technol.* 171, 274–284.

557 Zhang, L., Sun, X., 2015. Influence of bulking agents on physical, chemical, and
558 microbiological properties during the two-stage composting of green waste. *Waste
559 Manage.* 48, 115-126.

560 Zbytniewski, R., Buszewski, B., 2005. Characterization of natural organic matter (NOM)
561 derived from sewage sludge compost. Part 1: chemical and spectroscopic properties.
562 *Bioresour. Technol.* 96, 471–478.

563 Zhu, W., Yao, W., Du, W., 2016. Heavy metal variation and characterization change of
564 dissolved organic matter (DOM) obtained from composting or vermicomposting pig
565 manure amended with maize straw. *Environ. Sci. Pollut. Res.* 23, 12128-12139.

566

567

568

570**Table 1.** The main physico-chemicals characteristics of the initial raw materials (dry weight
571basis).

Parameters	Palm waste	Goat manure
pH	6.10 ± 0.18	8.02 ± 0.25
CE (µS cm ⁻¹)	2.01 ± 0.22	9700.00 ± 5.00
Dry matter (%)	18.30 ± 0.27	92.20 ± 0.53
Organic matter (%)	91.90 ± 0.55	64.65 ± 0.82
Organic carbon (%)	53.30 ± 0.55	37.50 ± 0.82
Total Kjeldahl nitrogen (%)	0.50	0.90
C/N	106.60	41.66
Phosphor (mg/g DM)	1.20	11.85
Mineral matter (%)	8.10 ± 0.55	35.34 ± 0.79
K ⁺ (%)	1.33	2.40
Ca ²⁺ (%)	1.11	0.18
Mg ²⁺ (%)	0.36	0.01
Na ⁺ (%)	0.15	0.00
Fe ²⁺ (mg/kg DM)	259	89.46
Zn ²⁺ (mg/kg DM)	6	0.35
Cu ²⁺ (mg/kg DM)	<5	0.12
Mn ²⁺ (mg/kg DM)	23	2.07

572 CE: Electrical conductivity, C/N: Carbon/Nitrogen; DM: dry matter.

573

574

575

576**Table 2.** The main palm waste and goat manure physico-chemical characteristics during co-
577composting.

Compostin							
g		MM					
duration	pH	CE	(%)	OM	C	N	C/N
(Day)		(mS cm ⁻¹)		(%)	(%)	(%)	

0	7.51 ± 0.06	2.71 ± 0.13	19.65 ± 0.49	80.35 ± 0.49	46.60	0.77	60.52
6	7.45 ± 0.05	2.70 ± 0.09	20.70 ± 0.85	79.30 ± 0.85	45.99	0.91	50.54
14	7.46 ± 0.08	2.86 ± 0.11	26.70 ± 0.85	73.30 ± 0.85	42.51	0.83	51.22
21	7.37 ± 0.13	2.78 ± 0.07	22.25 ± 0.49	77.75 ± 0.49	45.09	0.87	51.83
28	7.36 ± 0.10	2.55 ± 0.14	24.30 ± 0.99	75.70 ± 0.99	43.90	1.08	40.65
33	7.42 ± 0.03	2.83 ± 0.06	23.10 ± 0.57	76.90 ± 0.57	44.60	0.84	53.10
42	7.41 ± 0.08	2.93 ± 0.06	23.65 ± 0.64	76.65 ± 0.64	44.46	0.85	52.30
62	7.33 ± 0.06	2.93 ± 0.10	24.90 ± 1.56	75.10 ± 1.56	43.56	0.93	46.84
84	7.08 ± 0.12	3.03 ± 0.16	26.55 ± 1.77	73.45 ± 1.77	42.60	0.90	47.33
119	7.16 ± 0.05	3.32 ± 0.06	29.50 ± 0.13	70.50 ± 0.13	40.89	1.01	40.48
133	7.25 ± 0.10	3.59 ± 0.04	28.90 ± 0.28	71.10 ± 0.28	41.24	1.10	37.49
190	7.12 ± 0.17	4.33 ± 0.06	49.05 ± 2.19	50.95 ± 2.19	29.55	1.42	20.81

578CE: Electrical conductivity; OM: Organic matter; MM: Mineral matter.

579

580

581

582

583

584**Table 3.** The DOM characteristics progress during the composting process.

Composting duration (Day)	DOC (mg C/l)	SUVA (x10 ⁻³)					
		254	269	280	E ₂ /E ₃	E ₂ /E ₄	E ₄ /E ₆
0	845.6	1.64	1.50	1.49	4.43	17.54	4.50
6	760.0	1.63	1.47	1.35	4.49	16.55	4.13
14	658.6	1.55	1.38	1.23	4.67	18.07	5.63
21	518.7	1.81	1.60	1.43	4.75	20.08	7.40
33	588.2	2.17	1.89	1.69	4.63	19.47	6.38
42	431.5	2.65	2.32	2.06	4.65	19.71	5.63
84	748.8	2.13	1.83	1.63	4.93	22.22	9.17
190	397.9	3.48	3.04	2.69	4.63	18.79	5.70

585 DOM: dissolved organic matter; DOC: dissolved organic carbon; SUVA: specific ultraviolet

586absorbance.

587
588
589
590
591
592
593
594
595
596
597

598**Table 4.** The mean infrared spectral bands related to the compost.

Wavenumber (cm ⁻¹)	Assignment
3200-3600	Hydroxyl stretching vibration of phenol, alcohol and organic acid and N-H vibrations from amines and amides
2850-2964	Aliphatic C-H group
1750-1600	C=O amount in the organic matter
1716	C=C stretching vibration of acids and ketones carboxyl groups
1620-1650	Unsaturated aromatic C=C or ketone acids
1540-1580	Amide II bands and carboxylic group, N-H deformation
1525	Lignin pic
1420-1450	Aliphatic C-H deformation
1380-1400	O-H deformation of phenolic structure, C-H deformation in cellulose and hemicellulose
1220-1270	C-OH stretching of aromatic groups
1003-1200	C-O stretching of polysaccharides
1112	C-OH stretching of aliphatic OH
720-590	Alcohol, OH out of plane bend

599
600
601
602

603

604

605

606

607 **Table 5. Evolution of the humification ratios during the composting process.**

Compostin g progress (Day)	Absorbance ratios et définit wavenumber		
	1_650/2_845	1_525/2_925	2_920/1_640
Initial	1.43	0.37	1.60
6	1.51	0.49	1.31
14	1.94	0.79	1.00
21	1.67	0.61	1.22
28	1.65	0.60	1.12
33	1.68	0.71	1.07
42	1.80	0.66	1.02
62	1.50	0.50	1.32
84	1.64	0.80	0.96
119	1.70	0.67	1.01
134	1.70	0.69	0.98
190	1.95	1.13	0.71

608

609

610

611

612

613

614

615

616

617

53

54

618**Table 6.** The palm waste and goat manure compost characteristics.

619		Parameters	Compost					
620	CE: Electrical	pH	7.12 ± 0.17	conductivity; DM:				
		EC (mS cm ⁻¹)	4.33 ± 0.06					
621	dry matter.	Moisture (%)	25.86 ± 1.11					
		Dry matter (%)	74.14 ± 1.11					
622		Organic matter (%)	50.95± 2.19					
		Total organic carbon (%)	29.55 ± 2.19					
623		TKN (%)	1.42± 0.00					
		C/N	20.81± 2.19					
624		Mineral matter (%)	49.05 ± 2.19					
625	Table 7.	Phosphor (g kg ⁻¹ DM)	10.24	Correlation matrix				
		K (g kg ⁻¹ DM)	88					
626	between physico-	Mg (mg kg ⁻¹ DM)	227	chemical and				
		Na (mg kg ⁻¹ DM)	127					
627	biological	Fe (mg kg ⁻¹ DM)	57	composted				
		Mn (mg kg ⁻¹ DM)	1.85					
628	materials.	Zn (mg kg ⁻¹ DM)	0.60					
		Cu (mg kg ⁻¹ DM)	0.78	Respiratio GI				
	pH	Germination index (%)	88.48 ± 0.52	n				
	pH	1						
	CE	-0,704	1					
	Température	-0,066	-0,012	1				
	OM	0,688*	-0,930	-0,067	1			
	C/N	0,735**	-0,848	-0,110	0,909**	1		
	Respiration	0,476	-0,488	0,734**	0,399	0,296	1	
	GI	-0,837	0,875**	-0,122	-0,753	-0,745	-0,524	1

629*: Correlation is significant at the 0,05 level (2-tailed).

630**: Correlation is significant at the 0,01 level (2-tailed).

631CE: Electrical conductivity; OM: Organic matter; GI: Germination index.

632

633

634

635

636

637

638

639

640

641

642

643

Figure captions

644**Figure 1.** Windrow and ambient temperatures evolution during date palm waste (2/3) and
645goat manure (1/3) co- composting.

646**Figure 2.** Respiration profile reflecting microorganism activity during composting process.

647**Figure 3.** The germination index progress during date palm waste and goat manure co-
648composting.

649**Figure 4.** The UV-visible spectra of the initial and final compost samples.

650**Figure 5.** Infrared spectra of various composting stage.

651T0: initial compost sample; T6: compost sample at 6 d ; T14: compost sample at 14 d ; T21:
652compost sample at 21 d ; T28: compost sample at 28 d ; T33: compost sample at 33 d ; T42:
653compost sample at 42 d ; T62: compost sample at 62 d ; T84: compost sample at 84 d ; T119:
654compost sample at 119 d ; T134: compost sample at 134 d ; T190: final compost sample.

655**Figure 6. (A)** Excitation-emission matrix (EEM) fluorescent spectra of the different DOM
656extracted from compost materials during co composting process expressed in days (d); **(B)**
657The ratio evolution of the red zone specific of humic substances to the total fluorescent area.

658 **Figure 7.** Excitation-emission matrix spectra of principal fluorescent components identified
659 by the PARAFAC analysis. (S1) component 1; (S2) component 2; (S3) component 3; (S4)
660 component 4.

661 **Figure 8.** Principal component analysis of the physico-chemical and biological parameters.

662 **CE:** electrical conductivity, **OM:** organic matter, **GI:** germination index.

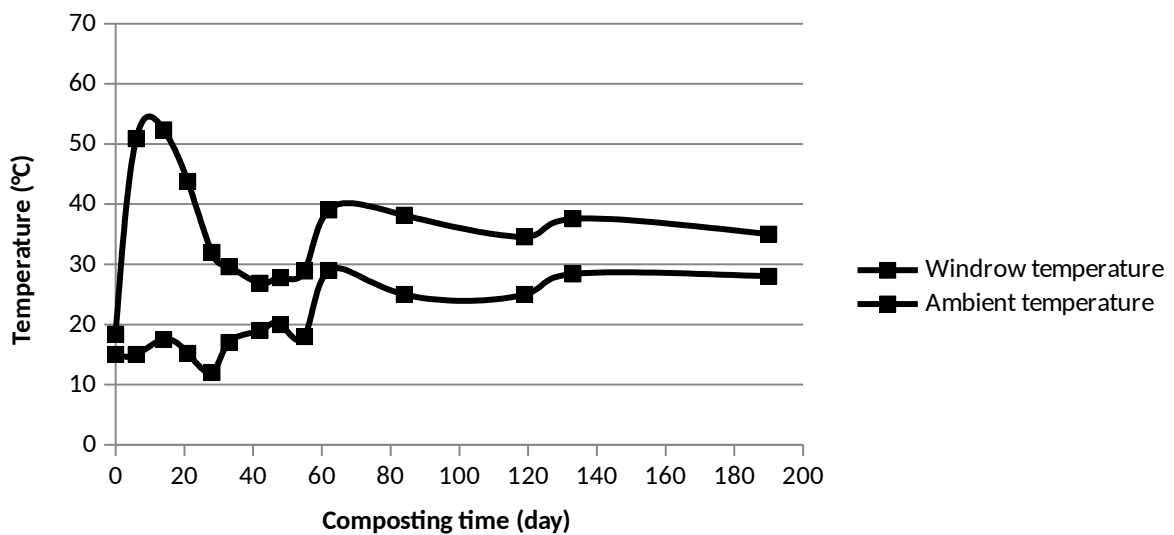
663

664

665

666

667

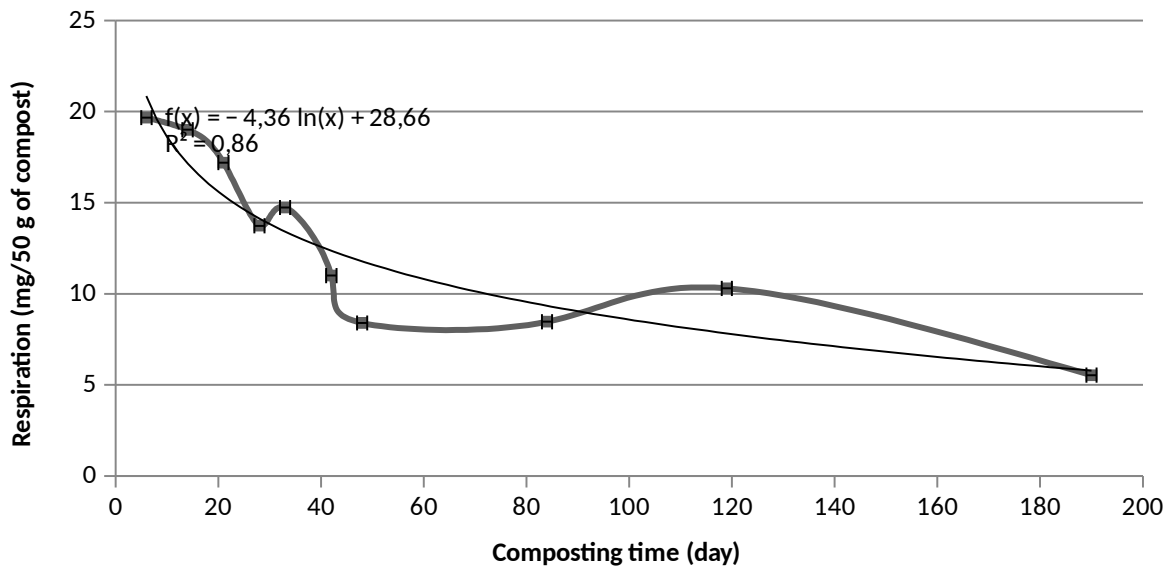


668

669

Figure 1

670



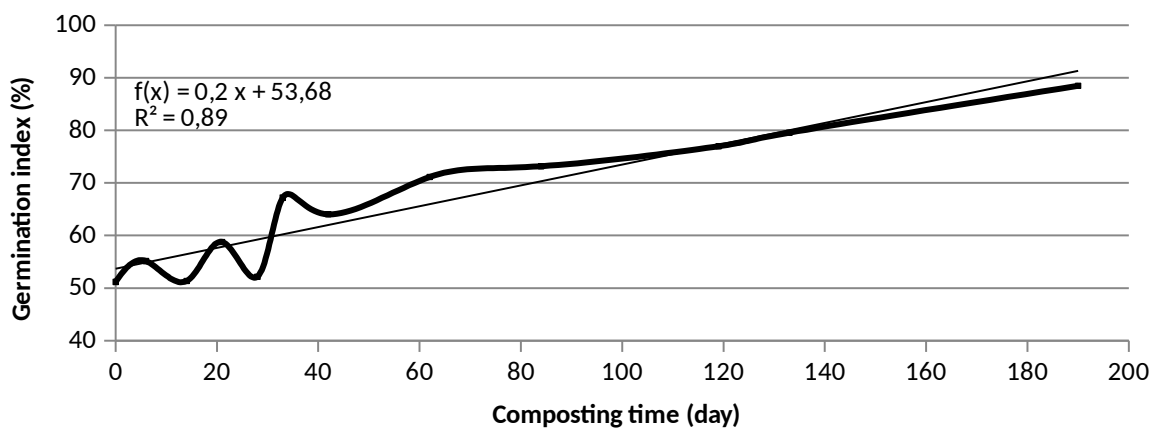
671

672 Ne pas mettre la ligne grise, laisser les points expérimentaux non relié. Préciser dans le
 673 texte que la corrélation n'est pas linéaire entre la respiration et le temps.

674

Figure 2

675

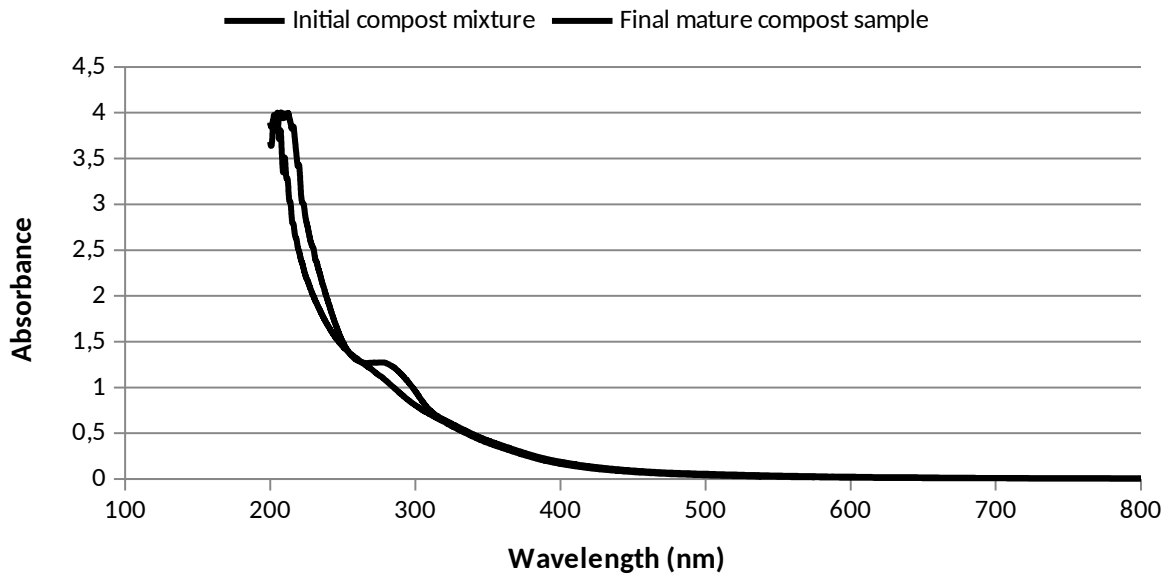


676

677 Figure 2 : Mettre les points de mesures sans ligne (ligne noire).

678

Figure 3



679

680 Le pic un peu avant 300 nm pourrait être dû au nitrate en fait !

Figure 4

681

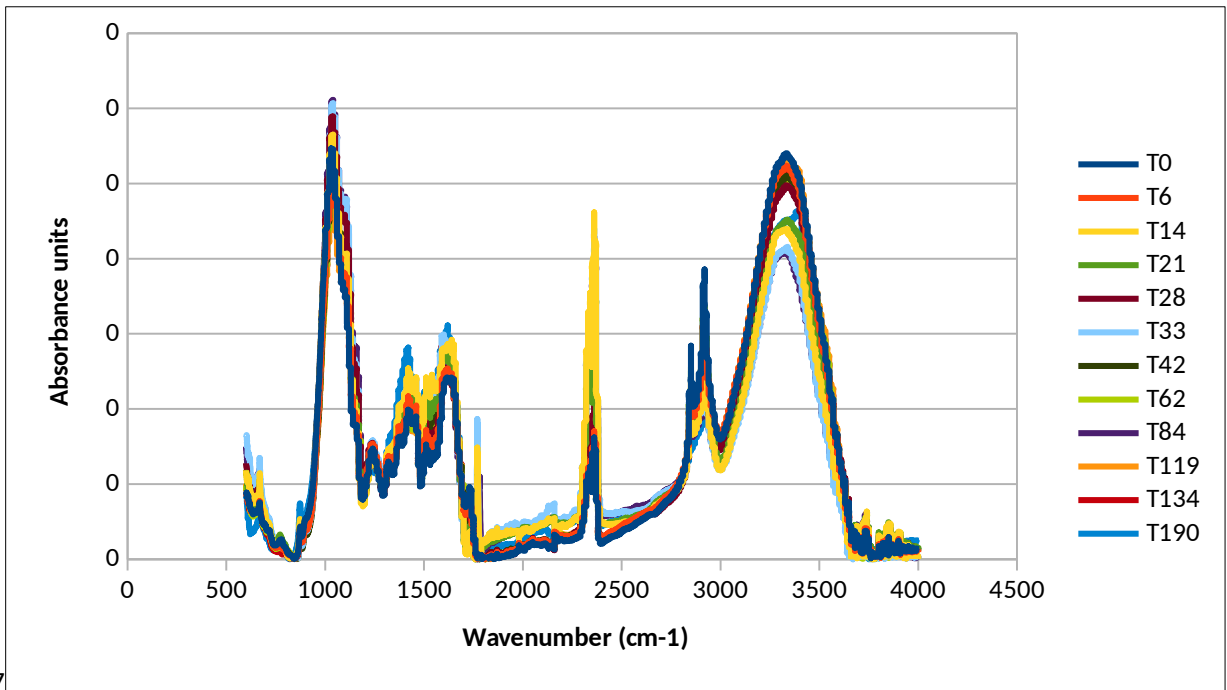
682

683

684

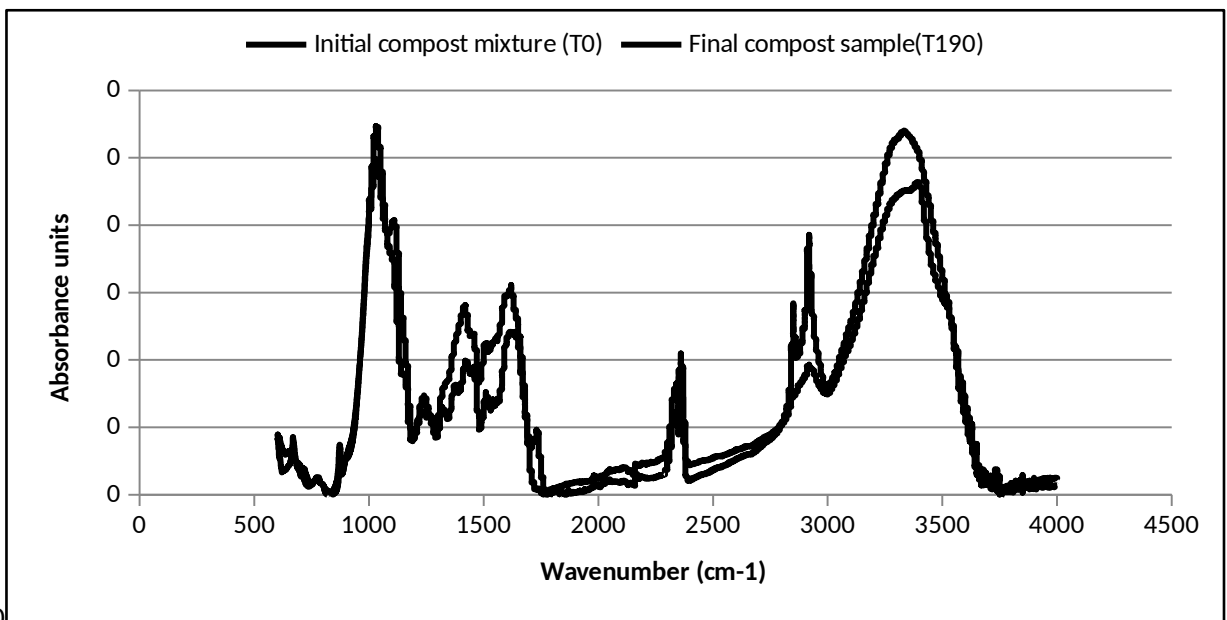
685

686



688A la place de la table 4 (pic IR) je mettrais les formules ou les noms sur le spectre, encore une fois si

689besoin seulement, le texte suffit à lui même je pense.



691

692

693

65

66

694

695

696

697

698

699

700

701

Figure 5

702

703

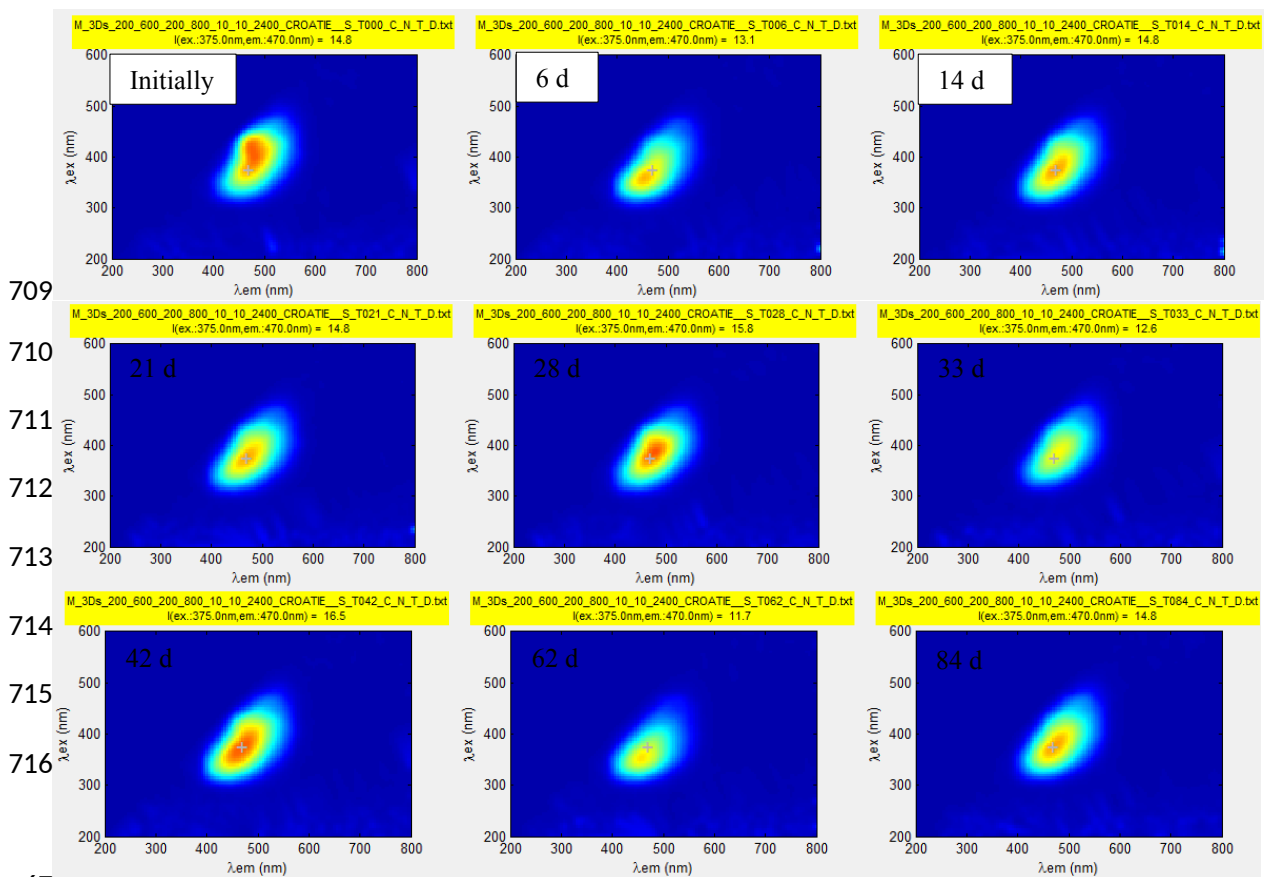
704

705

706

707

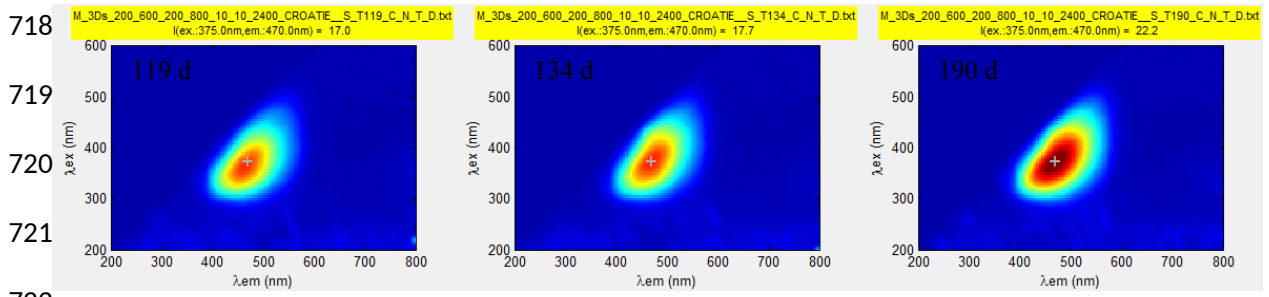
708(A)



67

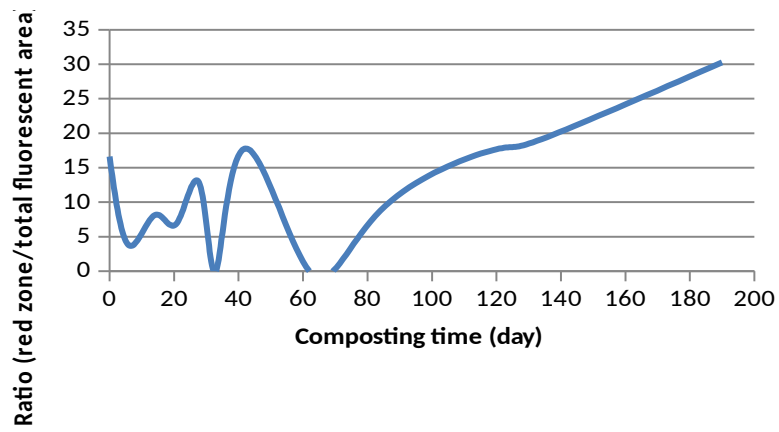
68

717



722

723(B)

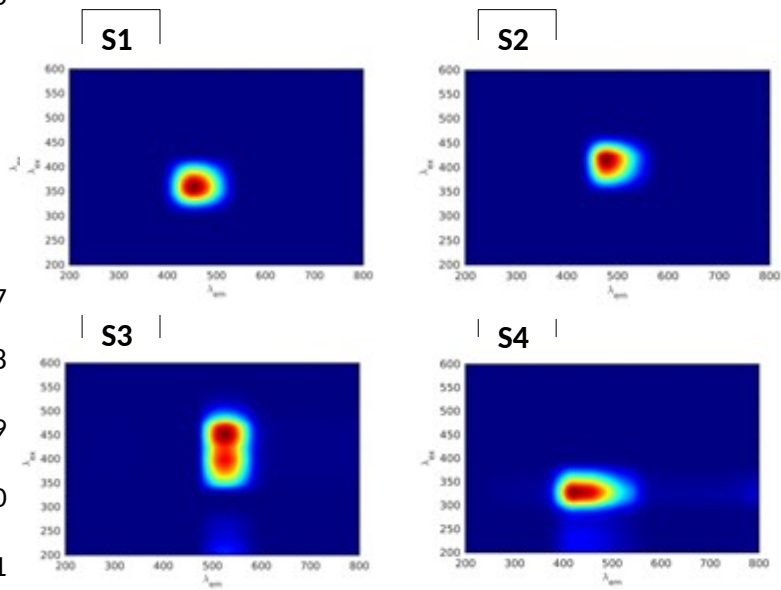


724

725

Figure 6

726



727

728

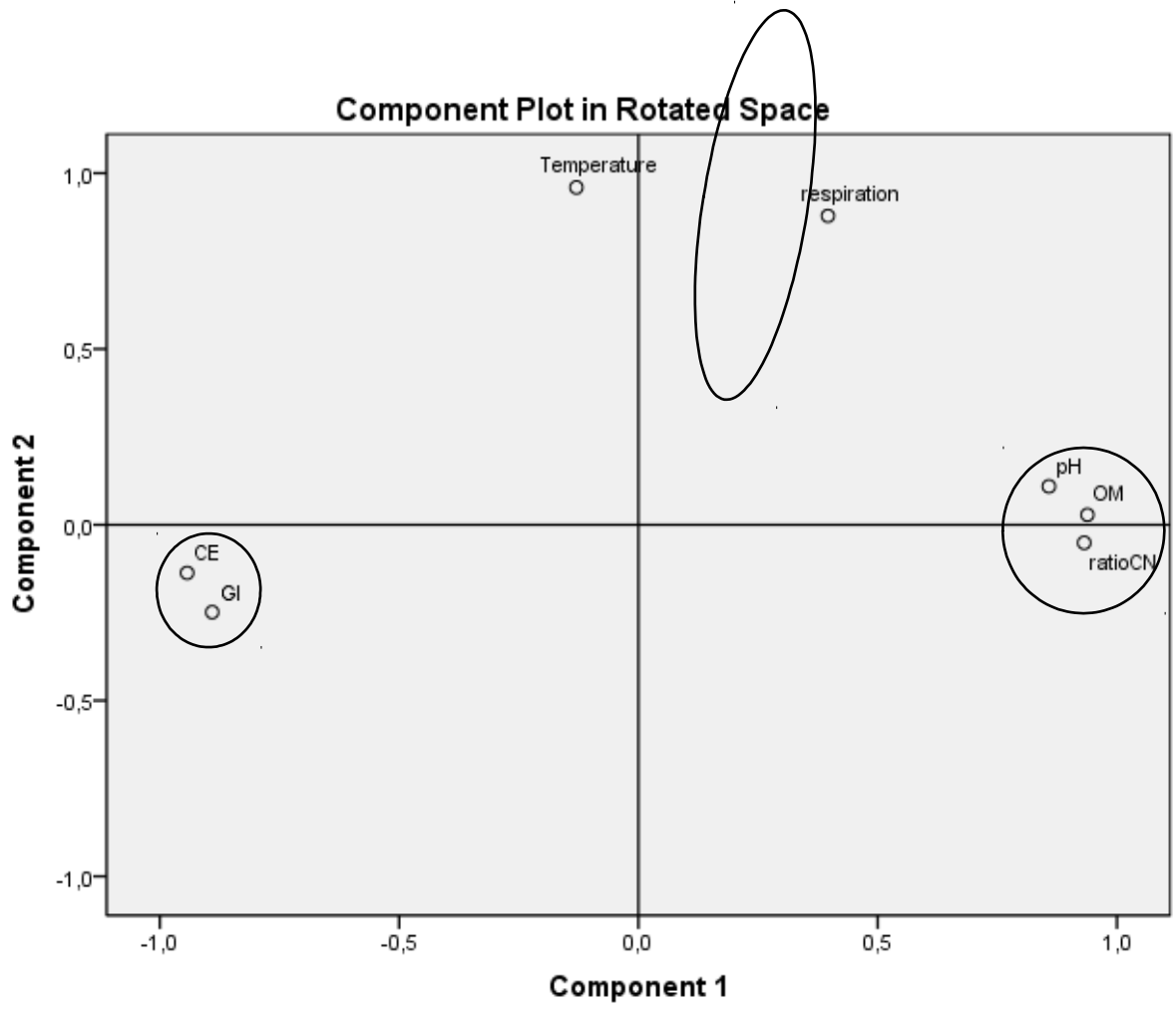
729

730

731

732

Figure 7



733

734

Figure 8